

doi:10.15199/48.2023.07.23

Performance and Losses Measurements of Switched Reluctance Motors with Powder and Laminated Magnetic Cores

Abstract. Article deals with measurements of performance and analysis of power losses of two switched reluctance motors with a soft magnetic composite core made of iron powder and a laminated Fe-Si steel core. The first one is a prototype motor whereas the second is a commercial one applied in washing machines. Both motors were supplied from a prototype controller. The commercial motor at low rotational speed develops higher torque and power than the prototype, whereas, inversely at high speed. Efficiency for prototype motor is higher for a whole range of rotational speed.

Streszczenie. W artykule przedstawiono wyniki pomiarów eksploatacyjnych i analizę strat mocy dwóch silników reluktancyjnych przełączalnych różniących się materiałem rdzenia magnetycznego. W pierwszym przypadku jest to proszkowy kompozyt magnetyczny, natomiast w drugim krzemowe blachy elektrotechniczne. Prototypowy i komercyjny silnik do pralki automatycznej były zasilane natomiast z prototypowego sterownika. Komercyjny silnik dla niskich prędkości obrotowych osiąga większy moment i moc niż silnik prototypowy, dla wyższych odwrotnie. Sprawność silnika prototypowego jest większa niż silnika komercyjnego dla całego zakresu prędkości obrotowych (**Pomiary parametrów eksploatacyjnych i strat mocy silników reluktancyjnych przełączalnych z proszkowym oraz blachowanym rdzeniem magnetycznym**).

Keywords: SRM, soft magnetic composite (SMC), motor performance measurements, power losses.

Słowa kluczowe: silnik reluktancyjny przełączalny, kompozyt magnetycznie miękki, pomiary eksploatacyjne silników, straty mocy.

Introduction

A drive with a switched reluctance motor (SRM) can be a real alternative for low power mainly universal motors for home appliances, DC or BLDC motors for electric bikes and induction motors for fans [1,2]. SRMs are one of the cheapest electric motors with many advantages in comparison to other types of motors [3]. They have high rotational speed, low loss especially at high speeds and high starting torque. What is more, SRMs do not have expensive permanent magnets, maintenance needed brushes and commutators. However the whole drive with a SRM needs a dedicated controller.

High efficiency of technical devices is nowadays one of the most important parameter of newly designed products. Electric motors are one of the most energy consuming group of machines. According to a report published by Global Efficiency Intelligence in 2017 electric motor systems consume 47% of all global energy consumption, whereas in industry, it is about 30%. The biggest industrial countries such as China, US, EU, India and Japan consume around 70% of all energy consumed by electric motors and drives.

Motors used in research

Two SRMs were measured and comparative analysis, of losses and efficiency was conducted. First one, a reference model H55BMBJL-1820 was built by Emerson Electric Co. and is dedicated for washing machines sold in the USA. That is why, configuration of coils has been changed from parallel to serial, so that the motor could be supplied from Polish supply system with AC voltage 230 V and compared with the prototype. In the further part of the article it will be named modified Emerson Electric motor (MEEM). The MEEM has a Fe-Si laminated steel magnetic core. The second motor has a composite magnetic core made of iron powder. The prototype motor was built in Lukasiewicz Research Network - Tele and Radio Research Institute. It has the same housing, bearings and shaft as the MEEM. The two motors during dynamic measurements were supplied from a prototype controller developed by Poznan University of Technology. This unit is composed of rectifier and asymmetric bridge converter. Powders that were used for manufacturing composite cores such as: Somaloy 700 and Somaloy 700 HR were supplied by Höganäs AB. The

prototype motor will be named in the further part of the article - powder magnetic motor (PMM).

Losses in magnetic cores

Calculation of losses in magnetic cores of electric machines is a very complicated task. For some types of motors it is easier to calculate iron losses than for other types of machines. For SRMs iron loss calculation is very difficult, because magnetic flux densities in different parts of the machine are distorted from sinusoidal curves and also in different parts of magnetic circuit they have different shapes and frequency [4]. Classical division of iron losses in magnetic circuits is into hysteresis losses taken into account static hysteresis loops, and dynamic losses. In general, hysteresis losses depend on an area of quasi-static hysteresis loop and frequency of magnetic flux, whereas classical dynamic losses (eddy current losses) depend on peak magnetic flux density and their frequency in power 2, resistivity, and thickness of material subjected to changing magnetic field. In turn, additional dynamic losses depend on the peak magnetic flux density, their frequency in power 1.5, and resistivity of material [5]. In design and prediction of electric motors behaviour this division is very complicated to be useful. Manufacturers of magnetic materials which are further composed into magnetic cores and circuits show in catalogues of materials often only specific total losses at defined peak magnetic flux density and their frequency. An empirical formula developed by Steinmetz is frequently used in practice to calculate iron loss in cores but is only valid for sinusoidal magnetic flux density.

Power losses in switched reluctance motors

Power losses in SRM drives cause deterioration of efficiency of the whole electric drive. It leads also to increase of demands for electric power in the supply system. Increasing power consumption also often causes emitting of CO₂ into atmosphere. That is why we are looking for electric drives with the lowest losses. Users of electric drives by decreasing losses in machines will pay less money during exploitation of drives.

Main losses in SRMs are losses in a magnetic core called iron losses and in an electric circuit called copper losses. Friction and windage losses occur also during

rotation of motor's rotor. Friction losses are caused by friction in bearings. In turn windage losses are caused by the salient rotor and are dependent on speed of a rotor.

Analytical calculations of iron losses in a SRM is practically impossible. There were developed a few models that deal with calculation of losses [4, 6, 7, 8]. All of them are so elaborate and difficult to apply in practice and calculate iron losses in a SRM stator and rotor core. That is why, Finite Element Method (FEM) is more often applied in calculation of iron losses [9].

Iron loss in SRMs can be decreased by application of newly developed soft magnetic materials with high resistivity and decreased losses in comparison to classical ones such as electrical steel sheets. For reduction of losses caused by eddy currents more often are applied powder cores such as soft magnetic composites (SMCs).

Powder magnetic composites

SMC (soft magnetic composite) cores are made of powder. They are more often applied in electric motors [10]. Powder used for cores are composed of at least two components: magnetic and current insulating. Mixture of components with desired composition, mostly magnetic powder up to even 99.8% and in small amount dielectric max. a few % by weight, is concentrated mostly in pressing dies with shape and dimensions of a desired product. Typically dimensions of magnetic powder grains are ranged from a few to a few hundred μm . After compression a dense product with about 95-97% of solid magnetic material is obtained. Iron is mostly used as magnetic powder, because it is cheap and has very good magnetic properties. Insulating material plays two roles, it ensures insulation of grains of iron powder from each other and binds magnetic powder to ensure high mechanical strength. Compressed magnetic core is further heated in a thermal chamber to ensure high strength of material with the temperature dependent on dielectric. As an example for epoxy resin temperatures are equal about 200°C .

Description of analysed motors

Fig. 1. shows a cross section of two analysed motors. Fig. 1 (a) is the modified Emerson Electric motor, whereas fig. 1 (b) the prototype one. Both motors have different core material and different coils. Both motors have the same stator core dimensions, only different rotors.

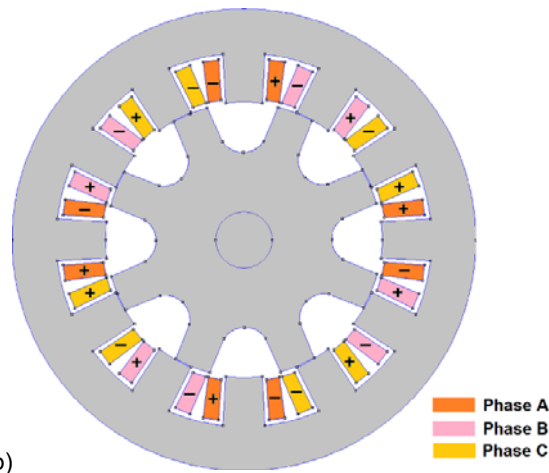
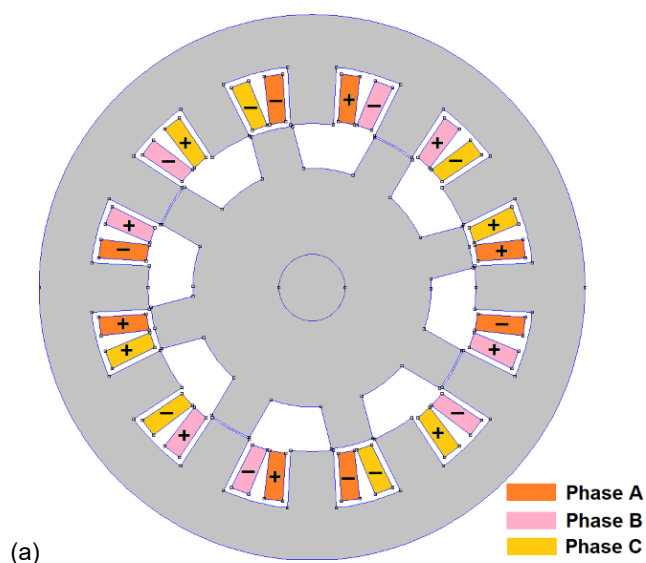


Fig. 1. Cross sections of 3 phase, 12/8, switched reluctance motors, (a) modified Emerson Electric, (b) prototype [11].

Table 1 shows the main parameters of SRMs.

Table 1. Parameters of the modified Emerson Electric motor and prototype with soft magnetic composite (SMC) core

Parameter	Modified commercial	Prototype motor
Nominal power	225 W	235 W
Base speed	2500 rpm	3000 rpm
Max. speed	9500 rpm	10000 rpm
DC supply voltage	310 V	310 V
External stator diameter	139.5 mm	139.5 mm
Axial length	47.3 mm	46.6 mm
Air gap	0.4 mm	0.25 mm
Stator core material	Fe-Si, 0.65 mm laminations	Somaloy 700
Rotor core material	Fe-Si, 0.65 mm laminations	Somaloy 700HR
Stator core mass	2.4 kg	2.3 kg
Rotor core mass	1.3 kg	1.2 kg
Coil turns	172	134
Wire diameter	0.56 mm	0.60 mm
Winding mass	0.78 kg	0.78 kg
Phase resistance	8.4 Ω	5.7 Ω
Phase inductance - aligned	228 mH	135 mH
Phase inductance - unaligned	36 mH	24 mH

Measurements of motors performance

Measurements of motors mechanical and efficiency characteristics and were conducted on a measuring stand shown in fig. 2.

The measuring stand is composed of the eddy current brake with Nd-Fe-B permanent magnets and aluminium disc, the torquemeter MW2006-3S type with the MT-3Nm sensor manufactured by Roman Pomianowski Pracownia Elektroniki, and a mechanical clamp. As a power analyser, U and I meter, there were used a digital power meter and analyser developed and manufactured by Poznan University of Technology, as well as the supply and controlling unit also developed by the same university. A digital thermometer was used for controlling temperature of windings and stator magnetic core by thermocouples placed on the stator and inside the coil.

Fig. 3 shows measured parameters of the drive with SRMs. Supply currents, voltage and power were measured by the mentioned power analyser. Rotational speed were measured by a meter included in the SRM controller. Phase currents were measured by a digital oscilloscope Tektronix TDS 210 with AC/DC current probe and with Fluke 115 multimeter.

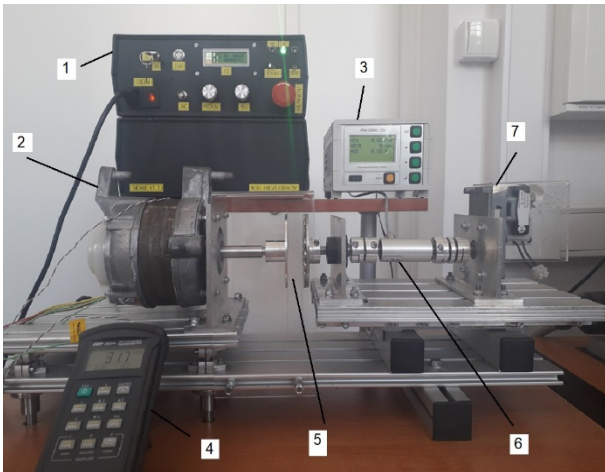


Fig. 2. Measuring stand for determination of mechanical parameters and efficiency of switched reluctance motors, 1 – supply and controlling unit, 2 – switched reluctance motor with the SMC core, 3 – torque meter, 4 – digital thermometer, 5- eddy current brake, 6 – torque sensor, 7 – mechanical clamp [12].

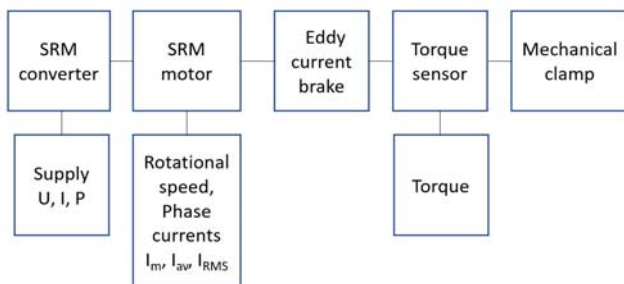


Fig. 3. A schematic diagram of measured parameters of the SRM drive.

In the first part of measurements static curves of electromagnetic torque were measured.

Fig. 4 shows measured electromagnetic torque vs. angle between rotor and stator poles for the MEEM and PMM motors for the same current linkages $\Theta=275$ A. This assumption enables to compare both motors with a different number of turns in coils. For the MEEM motor $I=1.6$ A, whereas for the PMM $I=2$ A.

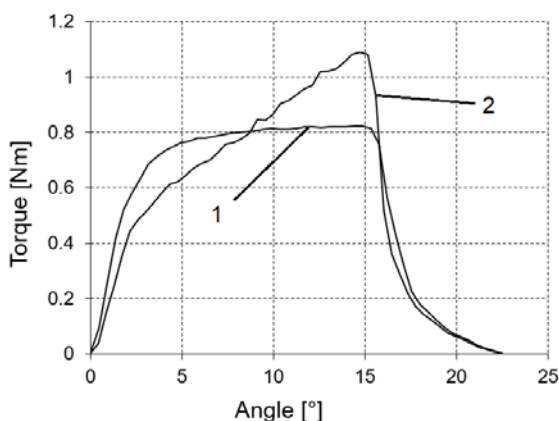


Fig. 4. Measured electromagnetic torque vs. angle between poles for modified Emerson Electric (1) and prototype (2) motors, $\Theta=275$ A.

As it can be seen from fig. 4 the PMM has higher maximum torque (1.09 Nm) in comparison to MEEM (0.82 Nm). The same situation is noticed for average torque.

Here the PMM also develops higher torque ($T=0.59$ Nm) than MEEM ($T=0.53$ Nm).

Fig. 5 shows torque vs rotational speed characteristics of the MEEM and PMM. For measurements shown in fig. 5 to 8 motors were supplied with $U_{DC}=310$ V.

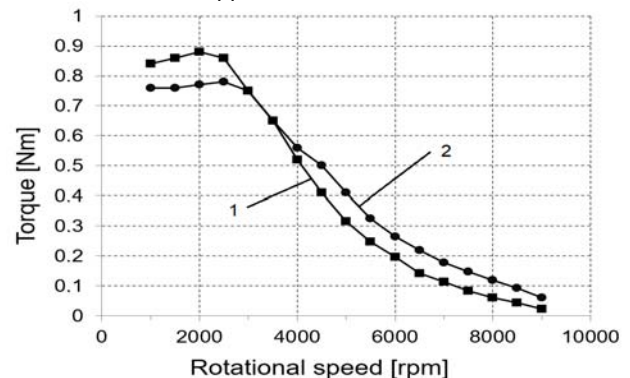


Fig. 5. Torque vs rotational speed curves of drives with the modified Emerson Electric (1) and prototype (2) motors.

As it can be seen from fig. 5 torque developed by the MEEM is higher than PMM for lower rotational speed up to 3500 rpm, whereas for higher rotational speed the situation changes. Maximum developed torque for the MEEM is almost 0.9 Nm, whereas for PMM almost 0.8 Nm. For both motors supplied from the same controller we can see that maximum rotational speed is 9000 rpm.

Fig. 6 shows mechanical power vs rotational speed curves of the MEEM and PMM.

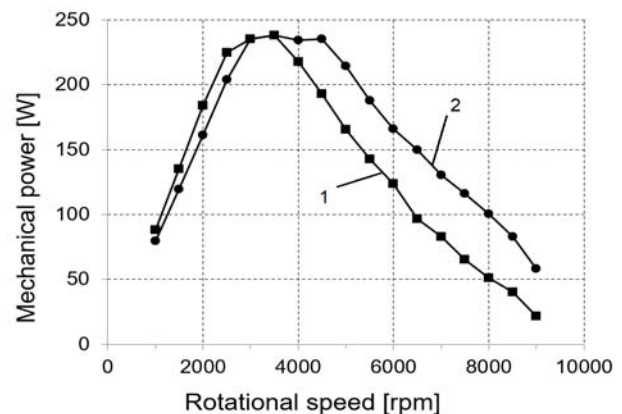


Fig. 6. Mechanical power vs rotational speed curves for drives with the modified Emerson Electric (1) and prototype (2) motors.

The same situation as in fig. 5 can be seen in fig. 6. Mechanical power for the MEEM is higher in a low speed range, whereas lower in the PMM above about 3500 rpm. Maximum available mechanical power for both motors is 240 W. For higher rotational speed the PMM develops higher mechanical power than MEEM. Difference between available power for rotational speed higher than 4500 rpm is equal about 50 W and is approximately the same up to 9000 rpm.

Fig. 7 shows curves of efficiency vs rotational speed of the MEEM and PMM. Efficiency of the drives were calculated by division of measurement of mechanical power on a motor shaft and measurement of electrical power supplying drives.

According to fig. 7 efficiency vs rotational speed of the PMM is higher than for MEEM for the whole speed range. Up to almost 4000 rpm the difference in efficiency is equal approximately 5%. For higher rotational speed the

discrepancy is higher and at 9000 rpm is 25%. Maximum efficiency for the PMM $\eta=76\%$, whereas for MEEM $\eta=72\%$.

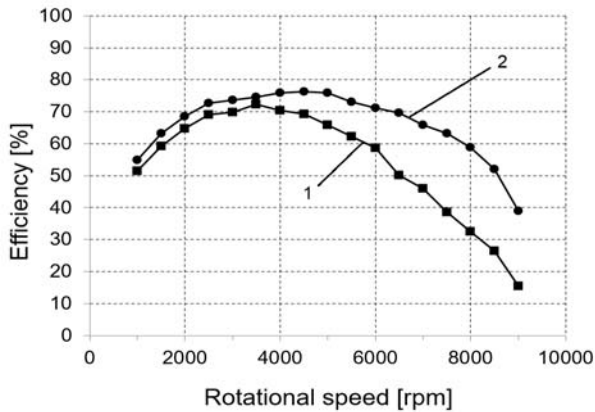


Fig. 7. Efficiency vs rotational speed curves of drives with the modified Emerson Electric (1) and prototype (2) motors.

In turn fig. 8 shows measured RMS supply current for both motors for conditions as for fig. 5-7. Here we can see that for rotational speeds lower than 4000 rpm the drive with the PMM consumes lower current. This situations changes for speed higher than 4000 rpm, where the PMM drive consumes higher current, but power, torque and efficiency is also higher. For both drives maximum current do not exceeds 2.4 A.

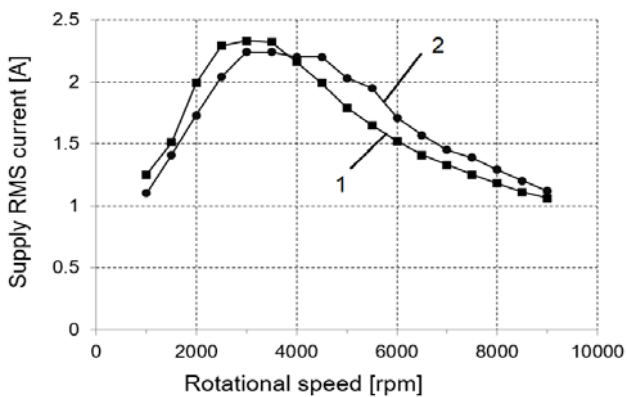


Fig. 8. Supply current vs rotational speed curves for the drive with the modified Emerson Electric (1) and prototype (2) motors.

Measurements of power losses in switched reluctance motors

In order to determine power losses in SRMs and their division into copper loss component, iron loss, and mechanical such as friction and winding loss, measurements of performance of the drive has to be conducted. Some power is lost also in the motor controller, its rectifier, and in asymmetric bridge converter. Calculation of such power loss is a very difficult task. According to simplified analysis conducted at maximum rotational power 240 W, in the converter maximum power lost in semiconductor elements such as an integrated rectifier bridge and MOSFET transistors is not higher than 4 W, for both motors, and decreases greatly when motor is not fully loaded. Power lost in the motor controller is not larger than 2% of maximum power. Power loss emitted in other parts of a supply circuit such as inductors, resistors are not taken into consideration.

Additional losses in SRMs are losses for friction in bearings and windage losses caused by a rotating rotor with

salient teeth. Winding and friction losses in bearings are often calculated using empirical equations which are true only for one type of motor with the same size. Here, friction and winding losses were determined together by measurements of rotational speed and torque of the SRM rotor for a speed range.

Fig. 9. shows the measuring stand for determination of winding and friction loss in the SRMs. A rotor of the SRM is rotated by a DC machine with controlled rotational speed.

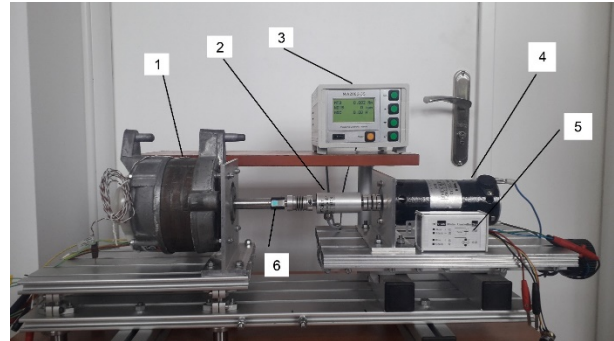


Fig. 9. Measuring stand for determination of winding and friction losses in the switched reluctance motors, 1 - switched reluctance motor with the SMC core, 2 – torque sensor, 3 – torque meter, 4 – DC motor, 5 – DC motor controller, 6 – optical reflective element for speed measurements.

The measuring stand is composed of the DC motor supplied from the DC motor controller with regulated speed from 0 to 4500 rpm. Rotational speed is measured by an optical tachometer made of Conrad Electronic, RC200 model, working with reflective element placed on a motor's shaft. In turn torque was measured also with the torque meter MW2006-3S, and sensor MT-3Nm as it was conducted for measurements of operational parameters of the motors.

Fig. 10 shows friction and windage losses in the MEEM and PMM.

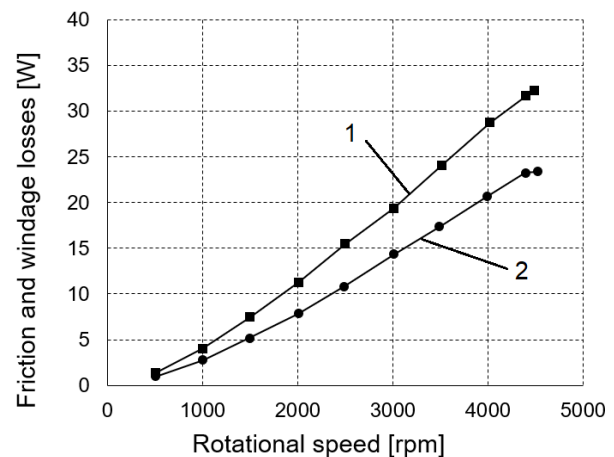


Fig. 10. Friction and windage losses vs rotational speed of modified Emerson Electric (1) and prototype (2) motors.

As it can be seen from fig. 10 mechanical losses in the MEEM are higher than in the PMM. It can be caused by thicker air-gap in MEEM, as well as a different construction of the rotor core. For lower rotating speed where friction loss is dominant discrepancy between curves is smaller than for higher rotating speed where windage losses are dominant.

Copper losses are emitted by the flow of electric current in windings of a motor. In the SRM this type of losses can be quite easily determined by measurement of RMS current in winding multiplied by resistance of wires [6]:

$$(1) \quad P_{Cu} = mI^2R_{Cu}$$

where: P_{Cu} – copper losses, m – number of phases in the SRM, I – RMS current value in the motor phase, R_{Cu} – phase resistance.

In SRMs calculation of losses in magnetic core is a very difficult task. In this paper iron losses were determined by subtraction other types of losses from input and output power:

$$(2) \quad P_{Fe} = P - P_o - P_{Cu} - P_W - P_F - P_E$$

where: P_{Fe} – power losses in the magnetic core, P – power taken from electrical energy source, P_o – output mechanical power, P_{Cu} – power lost in copper wires, P_W – power lost for windage of the rotor, P_F – power lost for friction in bearings, P_E – power lost in the electronic controller of the motor.

According to equation (2) iron loss was determined. In calculation it was assumed that P_E is equal zero and power for windage and friction was treated as an one component.

Analysis of losses in switched reluctance motors

In order to determine components of losses in the SRM the load test is needed to be done. In this measurement we determine input power, output power and copper loss. Iron loss is then calculated from subtraction of output power, copper loss, friction and windage loss from input power.

For comparison purpose measurements of material parameters of cores were also conducted.

Fig. 11 shows DC magnetization curves of materials that was used for magnetic cores in motors. For the prototype motor only curve for Somaloy 700 was shown, because Somaloy 700HR material is almost identical in magnetic properties.

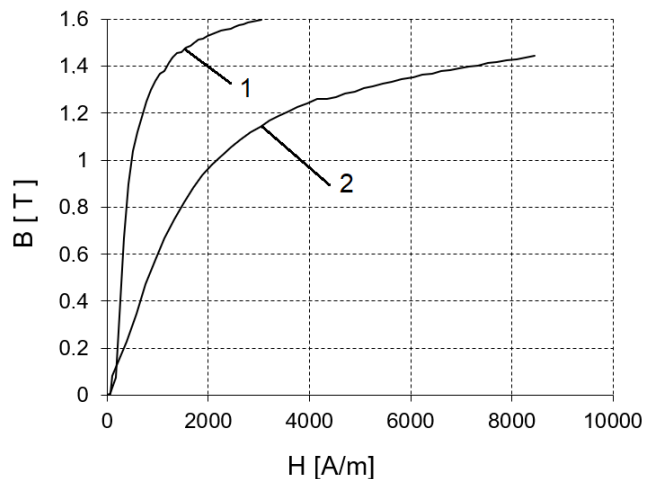


Fig. 11. DC magnetization curves of materials from the modified Emerson Electric (1) and prototype (2) motors.

According to data shown in fig. 11 electrical steel from MEEM has better magnetizability in comparison to Somaloy 700 material from the PMM. Maximum permeability for electrical steel $\mu=1600$, whereas for Somaloy 700 $\mu=500$.

Fig. 12 shows in turn iron losses vs magnetic flux density for both materials for $f=530$ Hz. This frequency was chosen in accordance with fundamental frequency for $n=4000$ rpm for 12/8 configuration of poles.

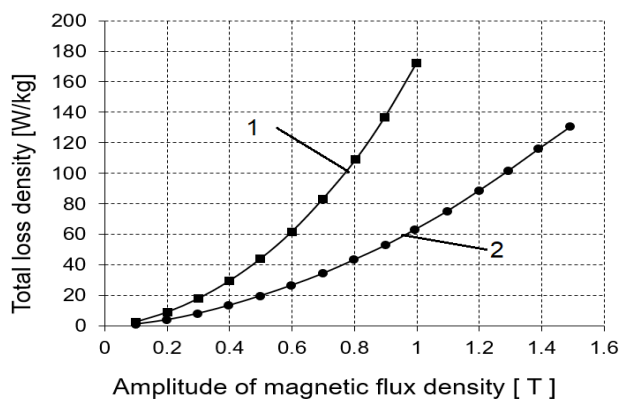


Fig. 12. Total loss density vs. magnetic flux density of materials from the modified Emerson Electric (1) and prototype (2) motors, $f=530$ Hz.

From fig. 12 we can see that electrical steel loss is higher than for Somaloy 700 material for $f=530$ Hz. For magnetic flux density $B=1$ T electric steel exhibits almost 3 times more total loss density than SMC material. Both fig. 11 and 12 were measured in Lukasiewicz Research Network - Tele and Radio Research Institute according to IEC standards.

For comparison of losses in the MEEM and PMM the same load of motors was applied. Table 2 shows measurement conditions of three load tests. Measurements were done at 3 different rotational speeds: 2000, 4000, 6000 rpm.

Table 2. Measurements conditions for determination of losses in modified Emerson Electric and prototype motors. Both motors have the same conditions.

Type of motors	Torque [Nm]	Speed [rpm]	Power [W]
MEEM and PMM	0.7	2000	147
	0.5	4000	209
	0.2	6000	126

Fig. 13 shows components of power losses for two analysed motors at rotational speed 2000 rpm, at the same load torque 0.7 Nm.

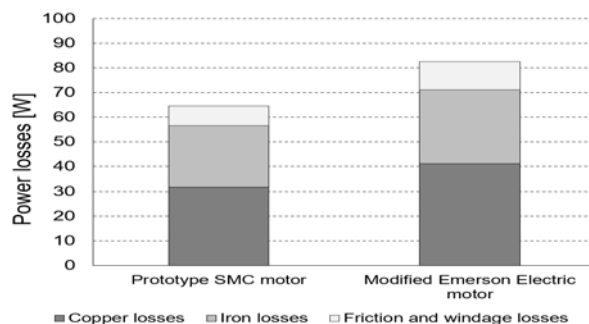


Fig. 13. Power losses for the prototype and modified Emerson Electric motors, $T=0.7$ Nm, rotational speed=2000 rpm.

As it can be seen from fig. 13 the biggest component of losses is copper losses, little smaller iron losses, and the smallest losses for friction and windage. Friction and windage losses are dependent of rotational speed that is why they are the smallest. Comparison of losses of motors show that the MEEM has larger power losses than the PMM. The MEEM has 28% larger total losses than PMM.

Fig. 14 shows results of measurements of power losses in the MEEM and PMM for load torque $T=0.5$ Nm and rotational speed $n=4000$ rpm.

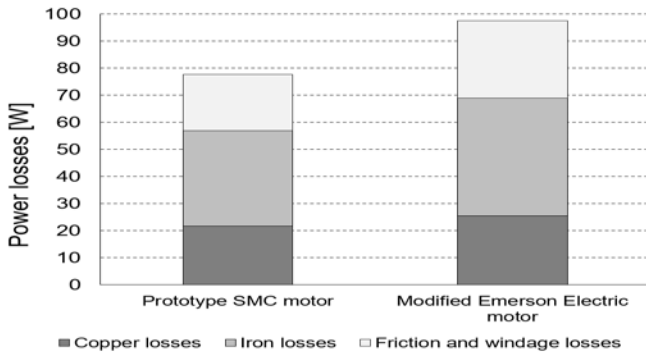


Fig. 14. Power losses for the prototype and modified Emerson Electric motors, T=0.5 Nm, n=4000 rpm.

Here we can see that copper losses are almost on the same level whereas winding and friction and iron losses and in MEEM are higher than in the PMM. Overall, MEEM has 28% higher losses than PMM.

Fig. 15 shows results of measurements of losses for the MEEM and PMM for load torque T=0.2 Nm, and rotational speed n=6000 rpm.

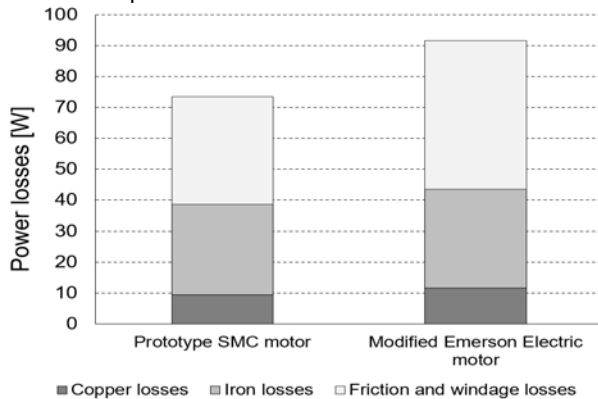


Fig. 15. Power losses for the prototype and modified Emerson Electric motors, T=0.2 Nm, n=6000 rpm.

We can here see that winding and friction losses are dominant part of losses. The remaining two components are almost on the same level. In this situation power losses in the MEEM are 25% higher than in the PMM. Power loss for friction and windage for rotational speed n=6000 rpm, (see fig. 10) were determined from the approximation and prediction of curves from 4500 to 6000 rpm. Approximation and prediction curves were conducted in Excel using polynomials in a second power.

Fig. 16-18 shows measurements of phase currents of both motors. Left curves are shown for the MEEM whereas right for the PPM. Both motors have the same courses of current. They differ only in values of currents.

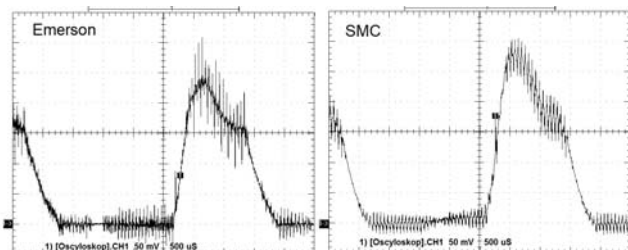


Fig. 16. Phase currents for n=2000 rpm, T=0.62 Nm, left: modified Emerson Electric motor, right: prototype motor, 1 div=0.5 A, 1 div=0.5 ms.

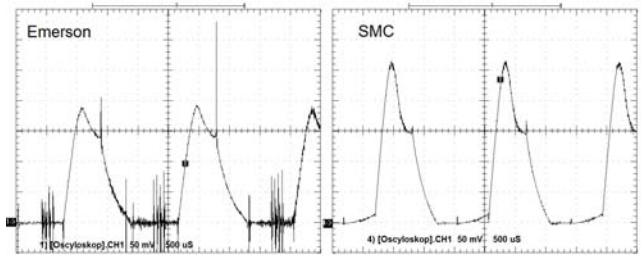


Fig. 17. Phase currents for n=4000 rpm, T=0.5 Nm, left: modified Emerson Electric motor, right: prototype motor, 1 div=0.5 A, 1 div=0.5 ms.

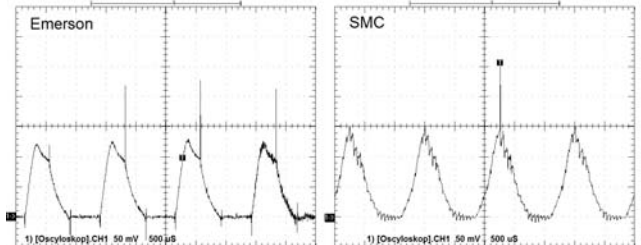


Fig. 18. Phase currents for n=6000 rpm, T=0.2 Nm, left: modified Emerson Electric motor, right: prototype motor, 1 div=0.5 A, 1 div=0.5 ms.

Table 3 shows measured currents for conditions as shown in fig. 16 to 18.

Table 3. Measured currents of modified Emerson Electric and prototype motors

Kind of motor	Torque [Nm]	Speed [rpm]	I_m [A]	I_{RMS} [A]	I_{AV} [A]
MEEM	0.62	2000	2.5	1.1	0.65
PMM			3.0	1.33	0.77
MEEM	0.5	4000	1.9	0.86	0.53
PMM			2.7	1.14	0.69
MEEM	0.2	6000	1.3	0.56	0.36
PMM			1.5	0.75	0.44

As it can be seen from fig. 16 to 18 the PMM has higher currents than the MEEM. Table 3 shows maximum, RMS and average values of currents.

Summary

Results of analysis and measurements have shown that the PMM can develop higher torque than the MEEM for rotational speed higher than n=3500 rpm, however for lower rotational speed than n=3000 rpm the MEEM develops higher torque. Both motors can obtain almost the same maximum mechanical power, approximately 240 W at the same n=3500 rpm. The PMM has higher efficiency in comparison to the MEEM for whole speed range from 1000 to 9000 rpm. Maximum efficiency for the PMM $\eta=76\%$, whereas for the MEEM $\eta=72\%$.

Results of determination losses in motors have shown that, for the same mechanical power, for analysed speeds n=2000 rpm, n=4000 rpm and n=6000 rpm, the PMM has lower total loss than the MEEM.

In the further research deeper analysis of core losses in both SRM will be conducted.

Author: dr inż. Marek Przybylski, Lukaszewicz Research Network – Tele and Radio Research Institute, ul. Ratuszowa 11, 03-450 Warszawa, E-mail: marek.przybylski@itr.lukasiewicz.gov.pl.

REFERENCES

- [1] Mynarek P., Gabor R., Kowol M., Kołodziej J., Łukaniszyn M., Analysis of a Modified-Structure Switched Reluctance Motor Designes for an E-Bike, *Przegląd Elektrotechniczny*, 95 (2019), No 5, 133-136
- [2] Bieńkowski K., Jackiewicz K., Kształtowanie charakterystyk mechanicznych dwufazowego silnika reluktancyjnego poprzez dobór kątów sterowania, *Przegląd Elektrotechniczny*, 93 (2017), nr 2, 13-16
- [3] Ahn J-W., Lukman G.F., Switched Reluctance Motor: Research Trends and Overview, *Ces Transcations on Electrical Machines and Systems*, 2 (2018), No. 4.,339-347
- [4] Torrent M., Andrada P., Blanque B., Martinez E., Perat J.I., Sanchez J.A., Method for Estimating Core Losses in Switched Reluctance Motors, *European Transactions on Electrical Power*, 21 (2011), No. 1, 757-771
- [5] Bertotti G., General Properties of Power Losses in Soft Ferromagnetic Materials, *IEEE Transactions on Magnetics*, 24 (1988), No. 1, 621-630
- [6] Materu P. N., Krishnan R., Estimation of Switched Reluctance Motor Losses, *IEEE Transactions on Industry Applications*, 28 (1992), No. 3, 668-679
- [7] Hayashi Y., Miller T.J.E., A New Approach to Calculating Core Losses in the SRM., *IEEE Transactions on Industry Applications*, 31 (1995), No. 5, 1039-1046
- [8] Raulin V., Radun A., Husain I., Modelling of Losses in Switched Reluctance Machines, *IEEE Transactions on Industry Applications*, 40 (2004), No. 6, 1560-1569
- [9] Ge L., Burkhard B., Doncker R. W. D., Fast Iron Loss and Thermal Prediction Method for Power Density and Efficiency Improvement in Switched Reluctance Machines, *IEEE Transactions on Industry Applications*, 67 (2020), No. 6, 4463-4473
- [10] Guo Y., Ba X., Liu L., et al., A review of Electric Motors with Soft Magnetic Composite Cores for Electric Drives., *Energies*, 16 (2023), No. 4
- [11] Przybylski M., Calculations and Measurements of Torque and Inductance of Switched Reluctance Motors with Laminated and Composite Magnetic Cores, *Archives of Electrical Engineering*, 71 (2022), No. 1, 125-138
- [12] Przybylski M., Ślusarek B., Di Barba P., Mognaschi M.E., Wiak S., Temperature and Torque Measurements of Switched Reluctance Actuator with Composite and Laminated Magnetic Cores., *Sensors*, 20 (2020), 1-14